Identifying the volcanic source of disconnected ash clouds using the HYSPLIT dispersion model *(NH23C-1538)*

Daniel B. Williams*, Michael S. Ramsey and Bobak Karimi

University of Pittsburgh, Department of Geology and Planetary Science

* Contact Author - dbw15@pitt.edu

Introduction

Monitoring of volcanic systems can provide insights into their hazard state. However, a large proportion of volcanic centers around the world are not actively monitored, with some capable of producing ash plumes in excess of 10 km high with little warning. These ash-rich plumes can become disconnected from the source, and the origin of these clouds can be difficult to determine if ground/satellite verification is not available. Here, a method is outlined for determining the volcanic origin of ash clouds, using a combination of remote sensing, backwards trajectory modelling, and geostatistical analysis to predict the source of ash clouds.

Methods

- **Satellite data of ash clouds were acquired for known eruptions of Etna (2002), Kliuchevskoi (2007), Chaitén (2008) and Ejyafjallajökull (2010) *[Fig. 1]*.**
- **Thermal infrared (TIR) image data used for this study were from the Moderate Resolution Imaging Spectroradiometer (MODIS), and were processed using the Brightness Temperature Difference (BTD) method of Prata (1989).**

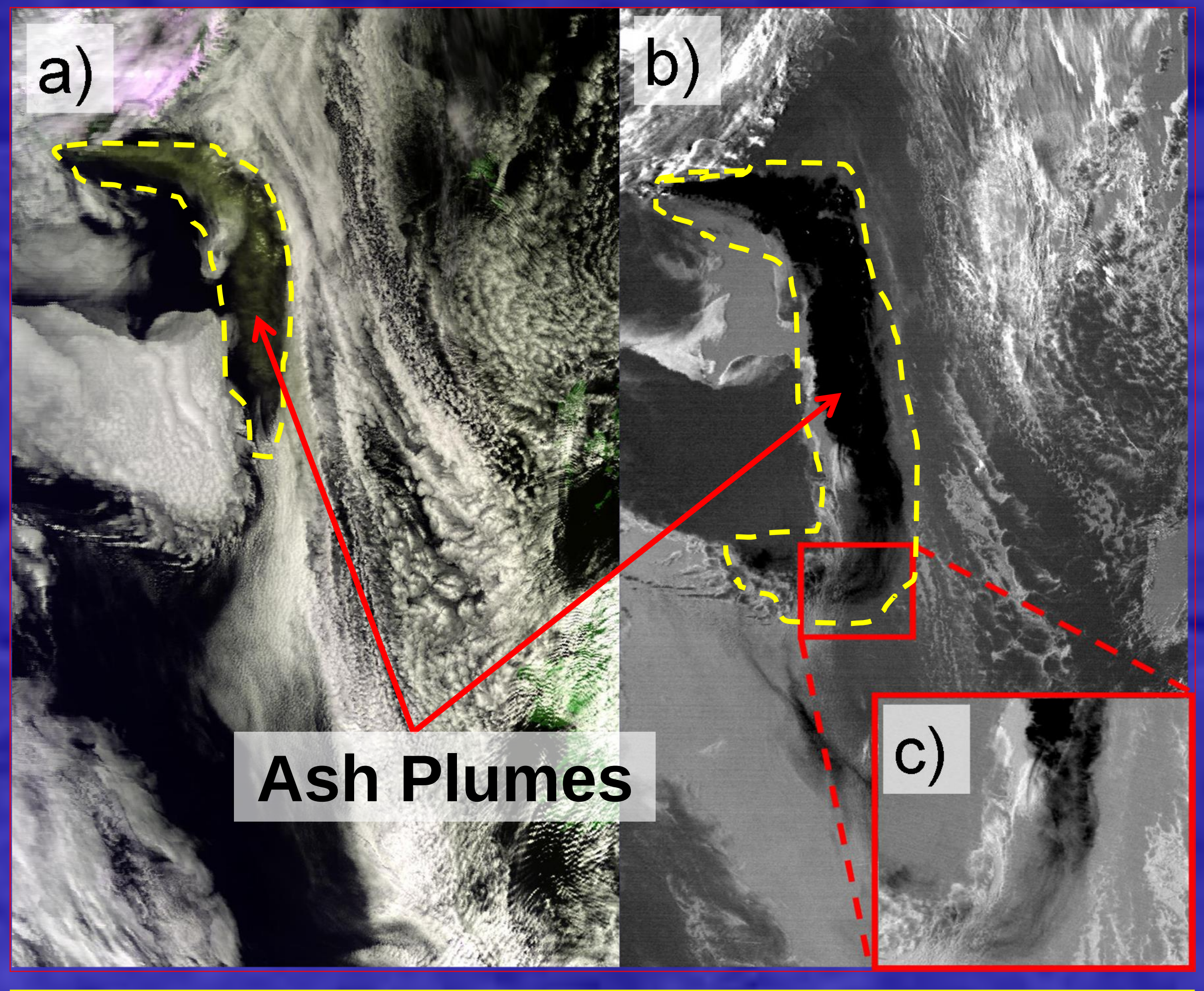

Figure 1. Image data from MODIS acquired on 6 May 6 2010 at 1155 UTC showing the full extent of the ash cloud in (a) visible and (b) TIR after performing BTD (Channel 31 – 32). An enlarged area of the distal portion (> 400 km from the vent) of the plume (c).

- **Ash cloud BTD images were gridded into cells using GIS and the coordinates of each cell were assigned density classifications based on the average BTD value.**
- **Back trajectories were calculated using the Hybrid Single Particle Lagrangian Integrated Trajectory (HYSPLIT) model (NOAA, 2013) at three height levels (troposphere, tropopause, and stratosphere).**
- **Kriging geostatistical method was applied to predict the regions of highest and lowest ash cloud density for each time step *[Fig. 2]*.**
- **Regions that were predicted as having the highest density for each step were used to create new, final trajectories.**
- **Likely sources were selected by distance to the trajectory.**

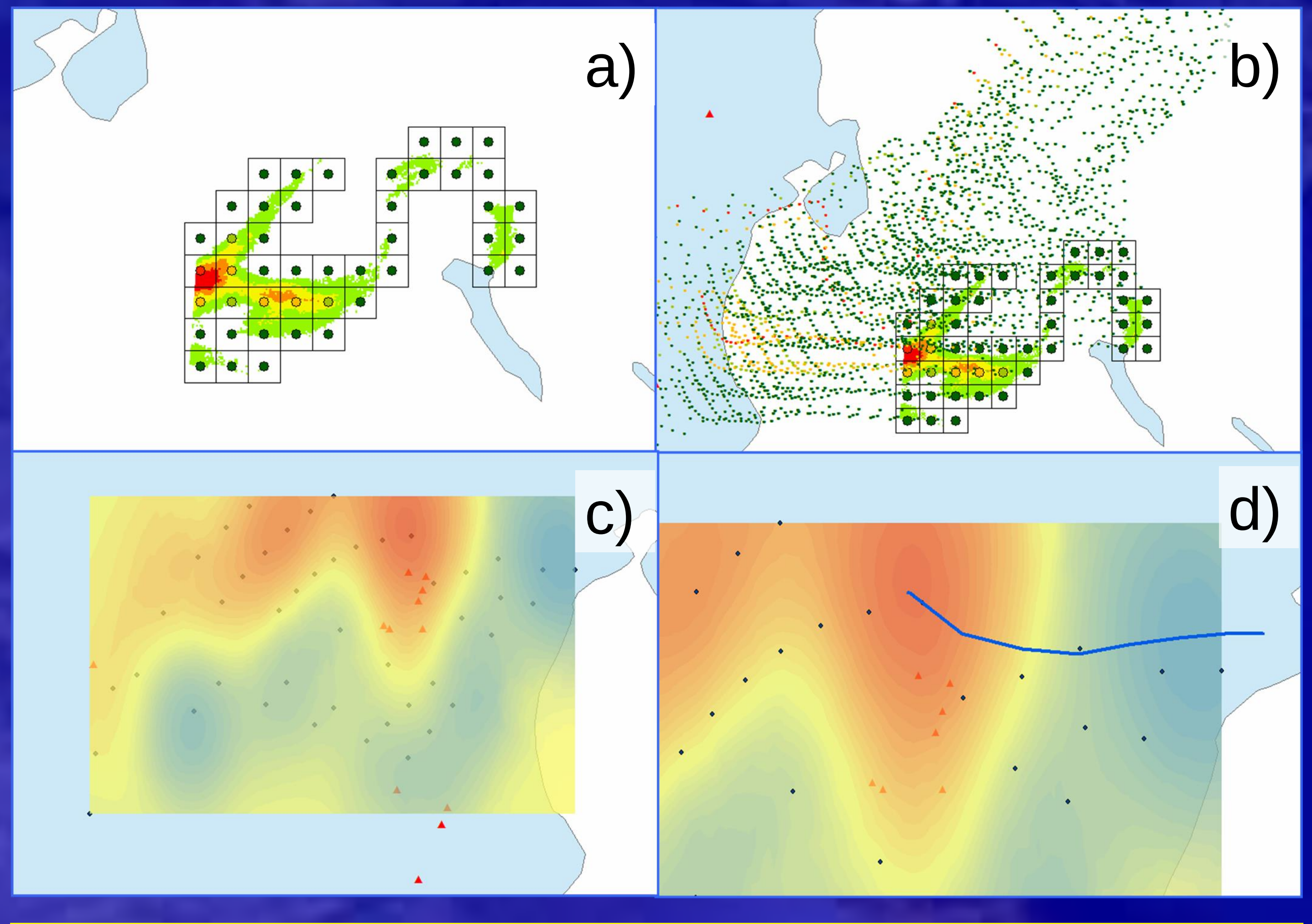

Figure 2. Example using the ash cloud from Kliuchevskoi (30 June 2007). a) A 50 x 50 km grid cell for this ash cloud, with different colors assigned to difference density values (Green = 1, Red = 5). b) All HYSPLIT trajectories and their starting locations at the three height levels. c) Kriging output contour plot at the tropopause height (Red = highest density, Blue = lowest density) of the cloud at 1100 UTC. d) the highest regions were connected together to form the final trajectory.

Results

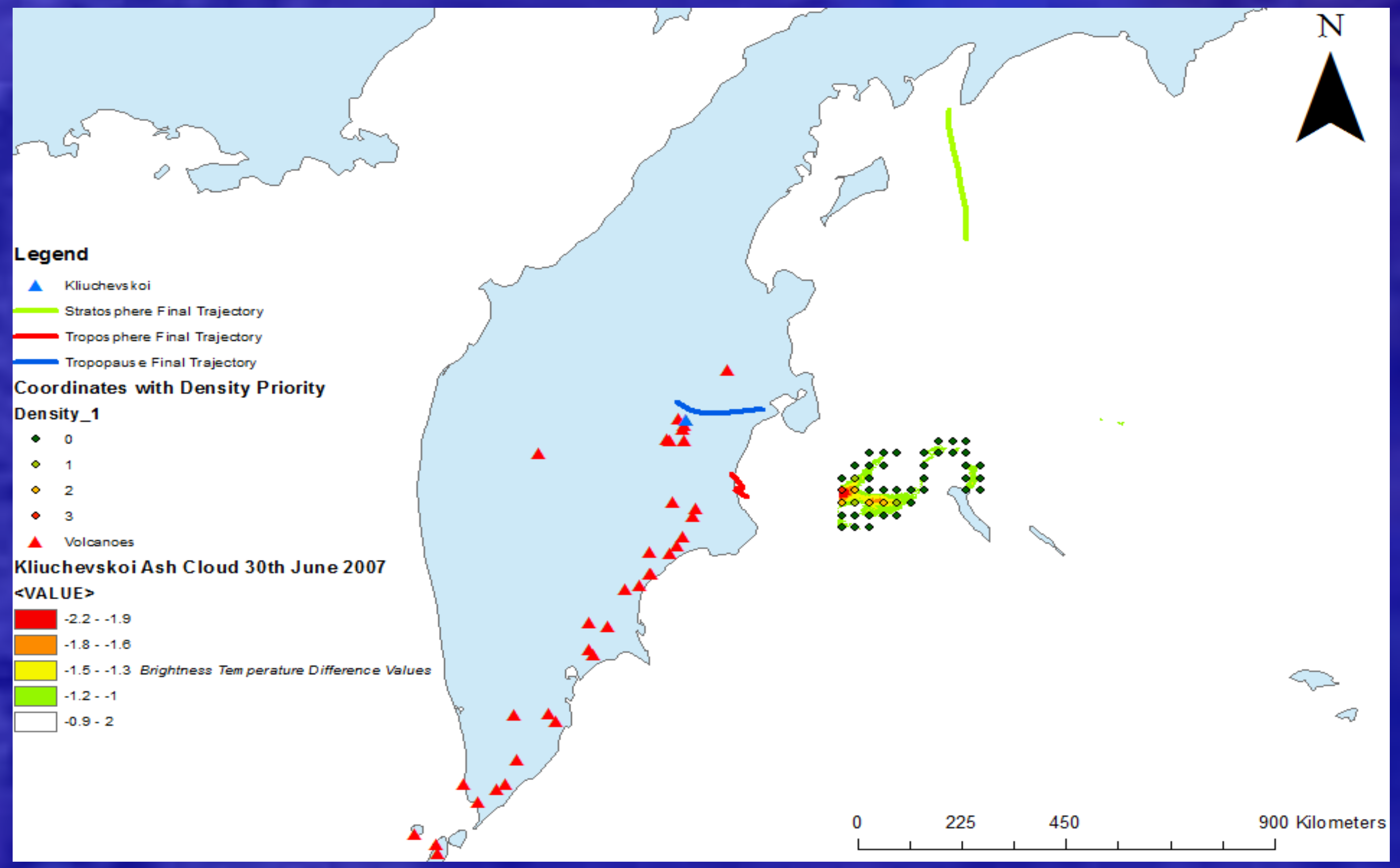

Figure 3. Ash cloud trajectory map for the 2007 eruption of Kliuchevskoi (Kamchatka, Russia). Trajectories represent the time span when volcanic centers were intersected. For this scenario, the closest correlation was with the tropopause height level came within 25 km of Kliuchevskoi between 1300 – 1200 UTC.

- **Results for this technique have all produced final back trajectories to within 100 km of the edifice at the tropopause.**
- **The tropopause provided the most accurate trajectory in all four examples, similar to results for other ash cloud transport models (Fero et al., 2009; Carey et al, 2008).**
- **Trajectory results for Etna, Kliuchevskoi, and Ejyafjallajökull range from 7 – 25 km from the vent, however this increases to 80 km for Chaitén *[Figs. 3 – 5]*.**
- **Work is limited by both the resolution of atmospheric models (Draxler and Hess, 1998; NOAA 2013), and the ability to detect ash clouds visually and using the BTD approach.**
- **Use of more sophisticated ash detection algorithms or different sensors, may enable greater accuracy in determining maximum cloud density.**

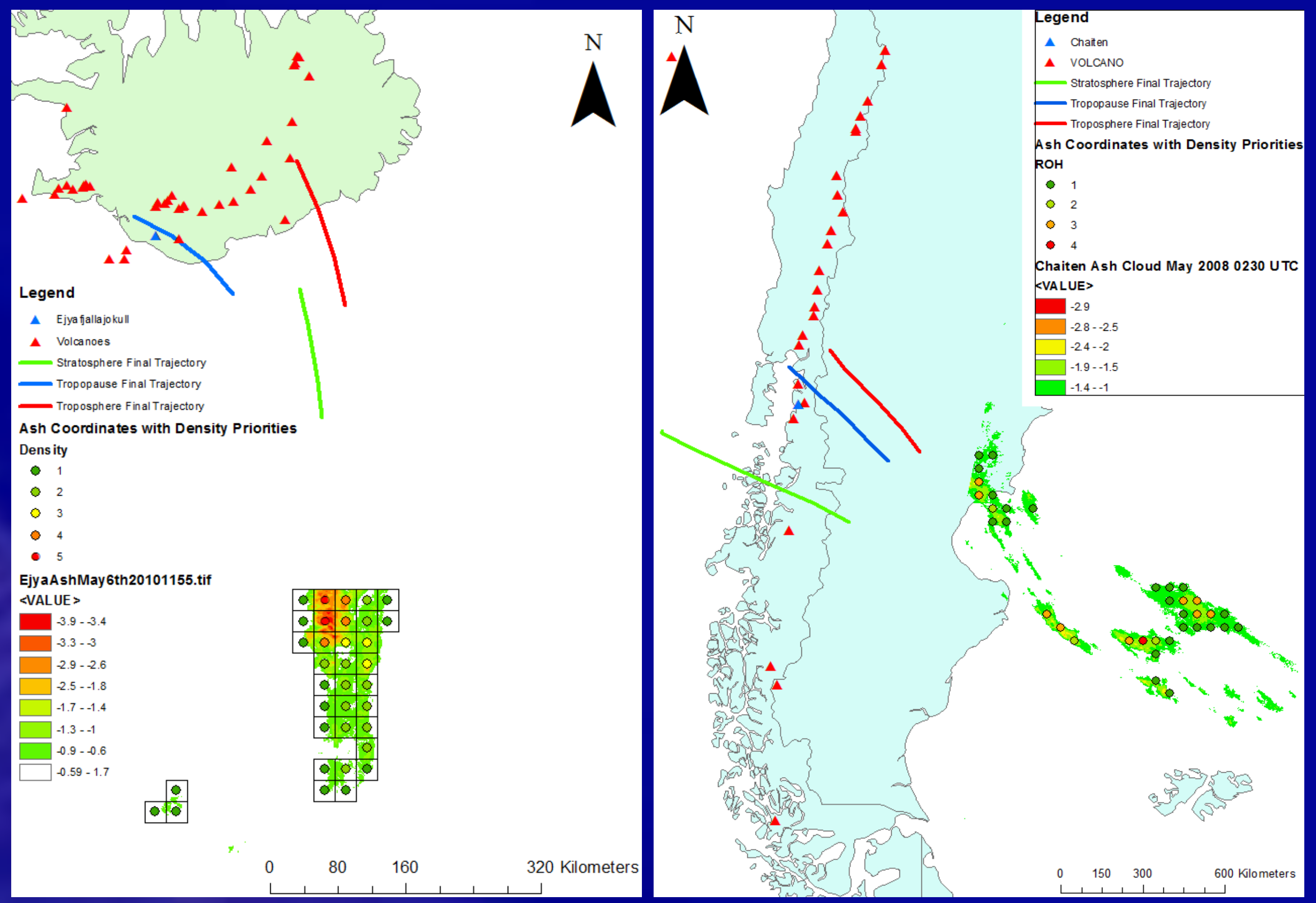

Figure 4. Trajectories for the 6 May 2010 Ejyafjallajökull eruption at 1155 UTC (left), and the 3 May 2007 Chaitén eruption at 0230 UTC (right). The Ejyafjallajökull cloud was between 400 and 500 km from the volcano, and the tropopause back trajectory was measured to within 7 km from the vent. The Chaitén cloud was between 755 and 2000 km from the source, and the tropopause trajectory was measured to within 80 km from the vent. This difference in vent proximity is likely due to the cloud at Chaitén being more diffuse as a result of its greater distance. By this point in time, the cloud may have been subject to micro-atmospheric turbulence that is beyond the range of HYSPLIT to model.

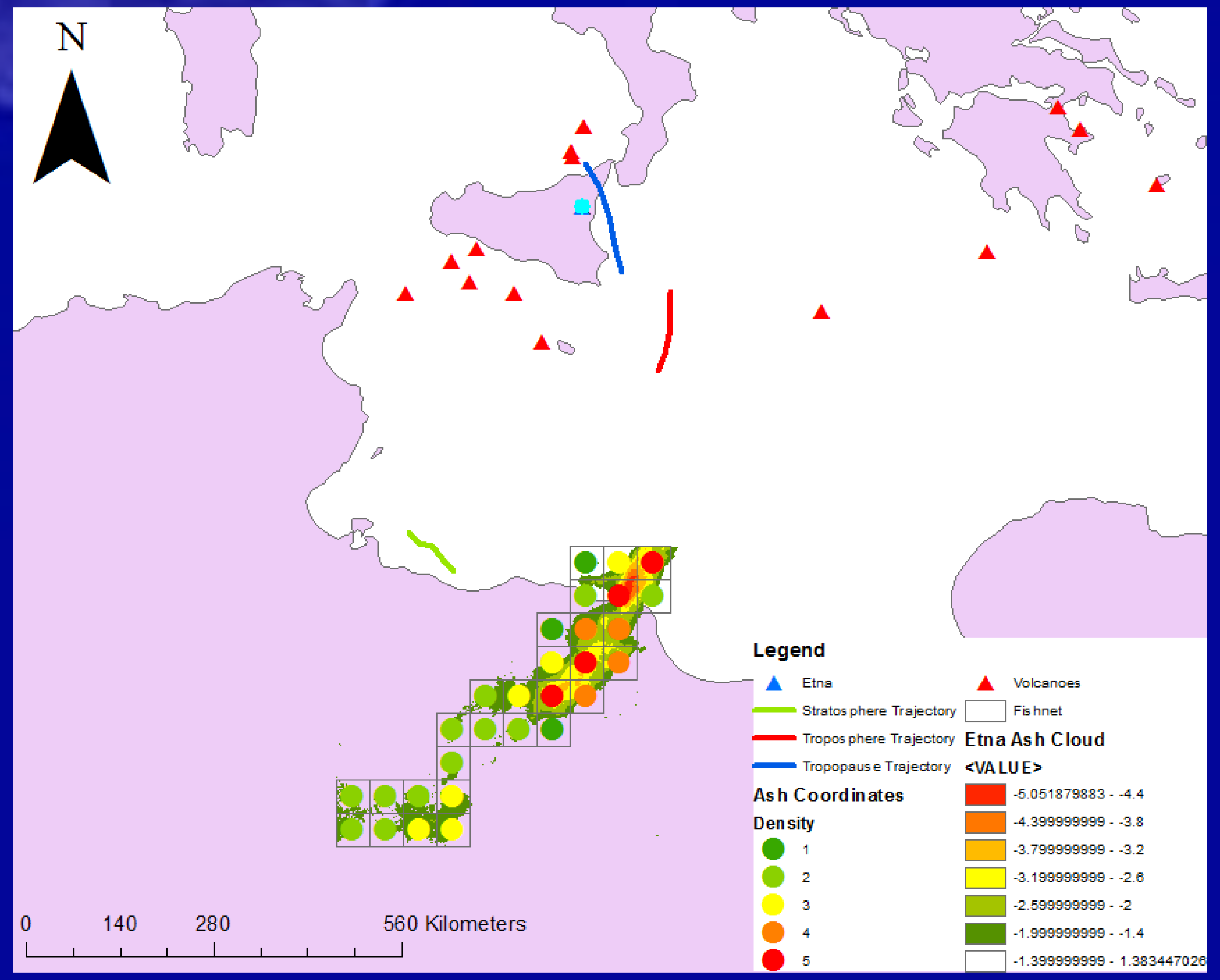

Figure 5. Results for the 1 November 2002 eruption of Mount Etna at 2145 UTC. The cloud was between 500 and 950 km from the vent. and the tropopause trajectory was tracked to within 12 km of vent.

Conclusions

The results of this preliminary and promising study have provided a geostatistical approach of back tracking disconnected volcanic ash clouds and potentially identifying their source. The next phase of this work will be to explore combining the results with other methods (e.g., thermal emission spectra, seismic records, etc.) to provide a more robust and accurate tool for eruption monitoring and hazard warnings. It is also expected that this work could strengthen existing back trajectory models, and aid in our understanding of the propagation of ash clouds in the atmosphere.

References

Carey S., Fero J. and Merrill J., (2008) Strong Influence of Near Tropopause Winds on Distal Volcanic Ash Transport, AGU Fall Meeting 2008, Abstract U33C-06

Draxler, R. R., & Hess, G. D. (1998). An overview of the HYSPLIT4 modeling system for trajectories, Australian Meteorological Magazine, *47*(4)

Fero J., Carey S. and Merrill J., (2009) Simulating the dispersal of tephra from the 1991 Pinatubo eruption: Implications for the formation of widespread ash layers, Journal of Volcanology and Geothermal Research, 186, 120-131

National Oceanic and Atmospheric Administration, (2013) The HYSPLIT users guide version 4, 209 pp.

Prata A.J. (1989) Observations of volcanic ash clouds in the 10-12 µm window using AVHRR/2 data, International Journal of Remote Sensing, 10(4), 751 – 761